

## 3-Amino-1,2,4-Triazole Tetramer: Electrical Conductivity Related To The Doped Degree

M. E. Lamanna<sup>2</sup>, E. DE LA Horra<sup>3</sup>, S. Jacobo<sup>3</sup>, N. B. D'Accorso<sup>1,2</sup>

<sup>1</sup>Centro de Investigaciones en Hidratos de Carbono (CIHIDECAR-CONICET).

<sup>2</sup>Dpto. de Química Orgánica, Facultad de Ciencias Exactas y Naturales. Universidad de Buenos Aires, Ciudad de Buenos Aires (1428), Buenos Aires. Argentina.

<sup>3</sup>Laboratorio de Físico Química de Materiales Cerámicos Electrónicos (INTECIN -CONICET), Dpto. de Química, Facultad de Ingeniería. Universidad de Buenos Aires.

**ABSTRACT:** A study on the electrical conductivity and thermal behavior of the new oligomer 3-amino-1,2,4-triazole tetramer, related to the doped degree and temperature in the range of  $300\text{ K} \leq T \leq 370\text{ K}$  has been performed. Sample doped in acid medium, at room temperature, showed the highest electrical conductivity ( $7.0 \cdot 10^{-3}\text{ S/cm}$ ), whereas neutral or basic samples presented two orders minor values of electrical conductivity. Morphological and structural characteristics are discussed. This new organic semiconductor can be prepared as a thin film in order to explore its optical properties. The results show that the energy at which absorption starts corresponds to the direct band gap at 1.7 eV. As the organic semiconductor OATA may be used to prepare large-area thin film and flexible device on low-price, flexible substrates by means of solution method, the authors deduce that this oligomer may have an important application potential in UV-Vis optoelectronic detecting or lighting field

**Keywords** - acid doping, 3-Amino-1,2,4-triazole tetramer (OATA), semiconducting polymers.

### I. INTRODUCTION

Organic semiconducting materials have been subject of intensive studies of many research groups [1, 2]; its molecular structure is characterized by extended  $\Pi$ -electron systems, which can be easily tuned by chemical substitution to give a large variety of such organic materials [3-6]. Among the available intrinsically conducting polymers (ICPs), polyaniline (PANI) is found to be the most promising because of its ease of synthesis, low cost monomer, tunable properties, and better stability compared to other ICPs. The synthesis of this material can be carried out by chemical or electrochemical oxidative polymerization [7, 8]. Organic semiconductor has a number of advantages over inorganic semiconductors, such as low price, light weight, large area, solution processing and flexible substrate, thus it is a promising material which may be used in optoelectronics ultraviolet device. That is one reason for studying and developing new organic ultraviolet semiconductors and devices. It is interesting to remark that this kind of conducting polymers have electronic semiconductor properties and, at the same time, the processing advantages and mechanical parameters of polymers.

The feature shared by all of them is originated from the common nature of their  $\pi$ -electron system, an enhanced conductivity in oxidized or in reduced state and reversible redox activation in a suitable environment. Among the conjugated polymers, heterocyclic polymers can become good semiconductors. In this way, Çelik and col. reported to fused heterocyclic compounds in polycrystalline thin films showed typical semiconducting characteristics [12]. Optical experiments provide a good way of examining the properties of semiconductors. Particularly measuring the absorption coefficient for various energies gives information about the band gaps of the material. Knowledge of these band gaps is extremely important for understanding the electrical properties of a semiconductor, and is therefore of great practical interest [13, 14].

In order to design new organic conducting materials, in previous paper we explored the polymerization of 3-amino-1,2,4-triazole by chemical oxidative reaction. We have reported a new oligomer (OATA) which was characterized as a tetramer that in preliminary studies showed semiconductor behavior [15].

In the present work we show the doping effect on the electrical conductivity, thermal and morphological properties of OATA. In addition, we explored a potential electrical application by the preparation of OATA thin films on glass support.

### II. EXPERIMENTAL

#### II.1 Materials and methods

All the reagents: 3-amino-1,2,4-triazole (ATA), ammonium persulfate (APS), hydrochloric acid (HCl), ammonium hydroxide (NH<sub>4</sub>OH) were obtained from commercial suppliers (Aldrich Co) and used without further purification. Powders and thin films casted on glass substrates were prepared by the synthesis of the oligomer of ATA in acidic media with four monomer units, as we previously described [14]. The thickness of the presented film was 690 nm and they were almost light amber in color.

#### II.2 Differential Scan Calorimetric (DSC)

The DSC measurements were performed on a TA Q series™ Q20-1041 and the program to run the samples was Advantage for Q Series Version 2.8.0.392, Thermal Advantage Release 4.8.3, Copyright(c) 2001 – 2007, TA Instruments - Waters LLC. The program analysis was carried on a TA Instrument Analysis 2000 for Windows 2000/XP, Version 4,4 A Build 4.4.05, Copyright (c) 1998 – 2006, TA Instruments - Waters LLC. Sample weights of 1.5–2.5 mg were used under a N<sub>2</sub> nitrogen atmosphere and introduced in aluminum pans. The equipment was calibrated with indium standard.

#### II.3 Morphological characterization

OATA powders were characterized by X-ray diffraction method using a Bruker D8 Advance diffractometer equipped with a Cu tube, Ge (111) incident beam monochromator ( $\lambda = 1.5406 \text{ \AA}$ ) and a Sol-X energy dispersive detector. The corresponding intensities were measured for  $2\theta$  angles from 10 to 70° with a step 0.02° and in the standard Bragg–Brentano geometry.

The morphological characterization of the samples was carried with a scanning electron microscope (SEM, Zeiss DSM982 Gemini). OATA powders were dispersed in an acid (a), basic (b) and neutral (c) solution and then, there were deposited onto a silicon substrate for SEM characterization. Morphological analysis of the OATA film prepared onto a glass substrate (d) is presented.

#### II.4 Electrical Measures

The neutral obtained material (N) was doped with different quantity of aqueous HCl solution (1M), (A) with different molar ratio OATA/HCl: 1:1, 1:2 and 1:3, or with ammonium hydroxide (1M) (B) in the ratio 1:3 by mixing OATA powders with these solutions with stirring for one hour. After these treatments the samples were dried at room temperature for 48h under vacuum.

Powders were pressed into pellets for electrical measurements. The pellets were 10 mm in diameter and 1.5-2.0 mm in thickness. For each doped sample, three pellets were tested and the conductivity of each pellet was measured in different directions.

The temperature dependence of conductivity was measured using a Wavetek digital multimeter and an oven with a controlled measuring system. The electrical contacts were made by silver paint. Measurements of the conductivity of all samples have been performed in the temperature range of  $300\text{K} \leq T \leq 370\text{K}$ .

Samples nomination is presented in Table 1.

**Table 1:** samples nomination

sample nomination	doped samples
N	without doping
A1	molar ratio OATA/HCl 1:1
A2	molar ratio OATA/HCl 1:2
A3	molar ratio OATA/HCl 1:3
B	molar ratio OATA/NH <sub>3</sub> 1:3

#### II.5 UV-Vis absorption spectra

Spectrophotometric measurements of the films were carried out using a Shimadzu UV-2401 PC spectrometer (spectral range of 300 to 700 nm) equipped with the corresponding software with the transmittance technique.

### III. RESULTS AND DISCUSSION

OATA presents in its structure several nitrogen atoms which can be involved in acid-base equilibrium [16]. Sample N shows a partially oxidized structure [15]. Figure 1 shows the proposed structures of the different samples (see Table 1) taking into account the different degree dopant.

The OATA, probably due to the presence of several nitrogen atoms, could be protonated or deprotonated according to the pH media. The net charge on these molecules is affected by pH of their surrounding environment and become more positively or negatively charged due to the loss or gain of protons (H<sup>+</sup>). These structural changes originate changes in the color and in the solubility behavior [16].

In order to relate the thermal behavior of these samples with its structure DSC analysis were performed. Figure 2 shows the experimental profiles.

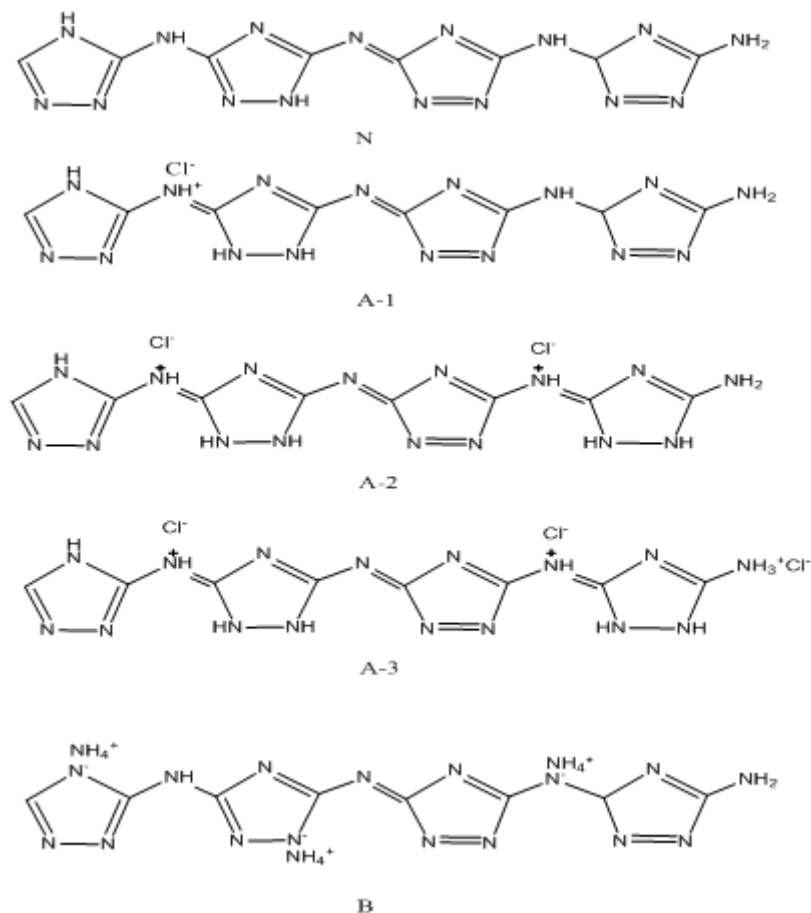


**Figure 1** Proposed structure of the different samples (see Table 1)

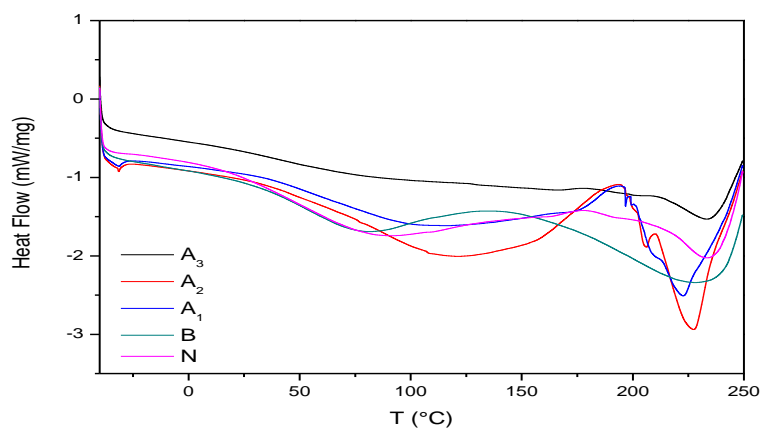


**Figure 2.** DSC results for all the studied samples.

All samples presented an endothermic peak between 210-230°C corresponding to the melting point. It is noticeable that samples A2 and A1 show a narrow peak related to a homogeneous structure. Furthermore, these samples present an exothermic peak before the melting temperature which could be assigned to a crystallization peak. Indeed, the glass Transition Temperature ( $T_g$ ) of the samples can be obtained from DSC analysis. In Table 2 we show  $T_g$  results obtained from OATA doped with different acid dopant (A1-A3) and from OATA (N) as a reference. It is well known that  $T_g$  values depend on the molecular weight and also depend on the molecular order. If the molecular weight is the only one considered, we expect that  $T_g$  values are incremented according to the increment on this variable so the order of  $T_g$  values would be:  $A_3 > A_2 > A_1 > \text{OATA}$ . However, A2 sample has the highest value.

**Table 2:** Tg results obtained from OATA doped with different acid dopant

Sample	Tg (°C)	MW increment (%)
A3	39	28.66
A2	88.4	18.95
A1	54.7	9.5
OATA	47.0	-

Tg: glass transition temperature. MW(%) mass increment of samples after doping

We can infer that the molecular weight is not the only one that affects the Tg values, also the molecular order plays a key role. So, the sample A2 is the one that showed the highest molecular order.

### III.1 Structural characterization

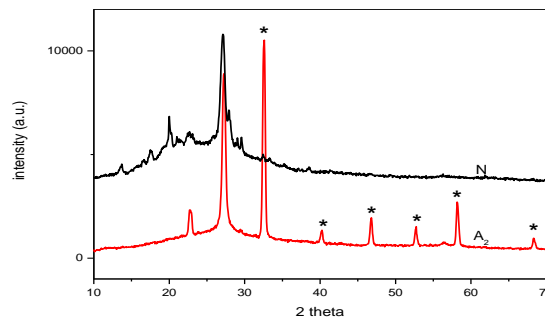
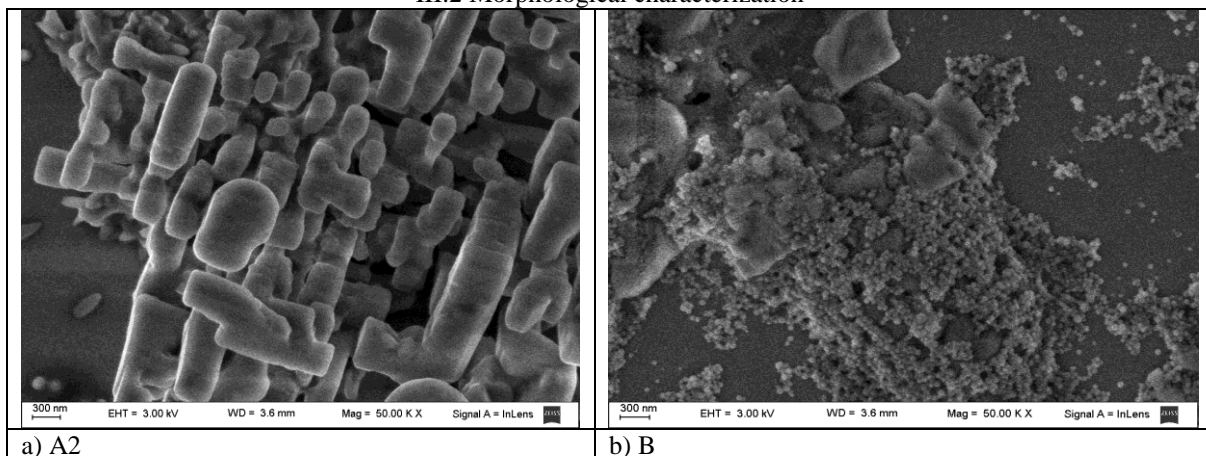
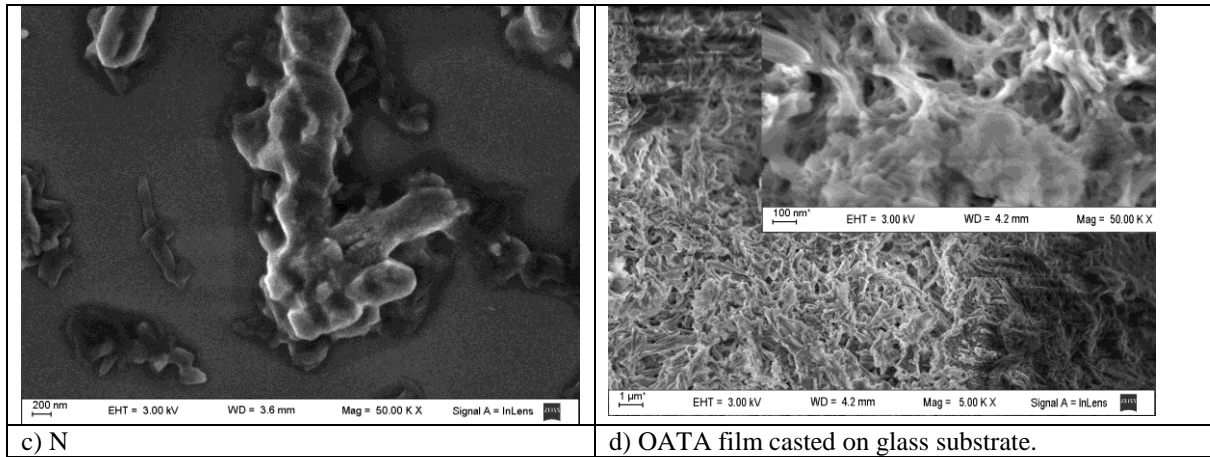


Figure 3: XRD of undoped OATA (N) and acid doped (A2) samples

We present in Figure 3 the x-ray diffraction patterns recorded for the undoped OATA (N) and acid doped (A2) samples. It is suggested that the diffraction pattern of a polymer with a high degree of crystalline order can be fitted with easily resolvable crystalline peaks and the intensity is related to the crystalline structure. Sample N exhibits broad peaks at  $2\theta = 20.0, 22.4^\circ, 27.2^\circ$  and  $2\theta = 29.1^\circ$  which can be attributed to the amorphous structure. For A2 the peak at  $20.0$  almost disappeared and the one placed at  $29.1$  becomes less intense. As OATA is a new oligomer, its DRX profile has not a special reference card so others similar structures were searched. The presence of the marked reflection peaks (\*) in the XRD pattern of A2 sample (Fig.3) is related to a hydrochloride salt (ref. code 00-022-1776)

### III.2 Morphological characterization





**Figure 4** Scanning microphotography's of OATA samples (powders) A2 (a), B (b) and N (c). OATA film casted on glass substrate (d) with two different magnifications.

The SEM micrographs of samples are shown in Figure 4. The difference between the three micrographs structures (a, b and c) is indicative of the influence of the dopant on the morphology of the samples. A2 sample (a) shows an ordered structure while the samples B and N show a random array. The thin film (d) shows a sponge-like structure (porous) which covers the entire substrate surface.

### III.3 Electrical Measures

Measurements of the conductivity of OATA with different dopant (pressed pellets) have been made in the temperature range of 300-370K where the oligomer shows good thermal stability [15]. They have been analyzed repeatedly, in all cases yielding reproducible results. It was observed that several parameters like doping level, time of drying and the medium of preparation have controlling influence on the conductivity of OATA samples.

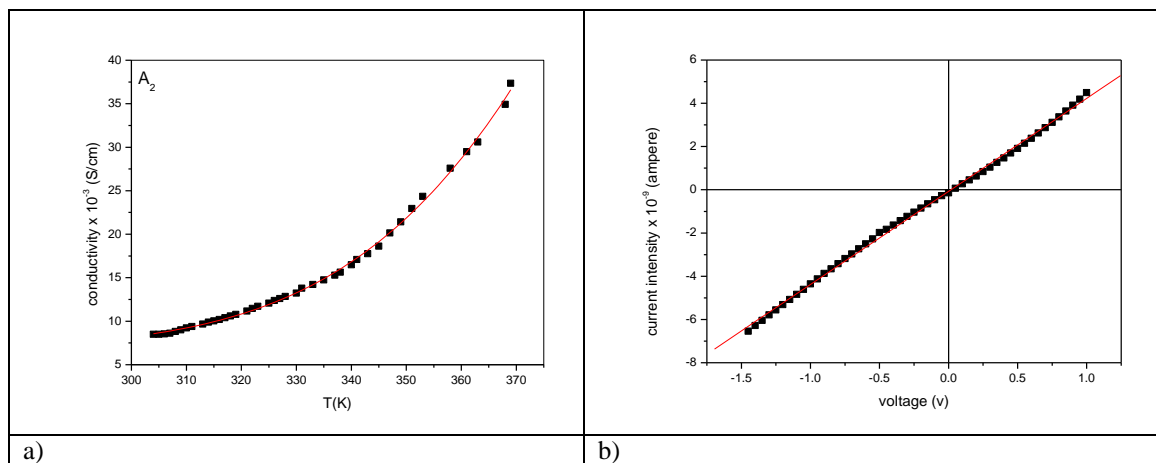


**Figure 5** a) Conductivity (S/cm) of A2 as a function of the temperature and b) Change of current intensity versus applied electrical tension for A2

All samples present a semiconductor behavior as conductivity increases with temperature. Figure 5a) show sample A2 profile as a function of temperature, experimental data was fitted by a Gaussian curve. Fig.5b) shows a linear behavior when sample (A2) is placed in an electrical field. Similar profiles were observed for each doped sample. These results are related to electronic conduction as in other well studied polymers as polyaniline [17], polipyrrol, etc. These results can be related to the proposal structures shown in Fig.1. Sample A2 show a total conjugated structure with the possibility of interchange interaction through the amine terminal group.

The consequences for the electrical conductivity as a function of temperature and of frequency were discussed by Holstein [18] and Mott [19].

At high temperatures the conductivity has a simple activated form:

$$\sigma(T) = \sigma_o \exp\left(-\frac{E_g}{2kT}\right) \tag{1}$$

where  $E_g = \frac{1}{2} E_a$ ;  $E_a$  is the activation energy for the small polaron hopping process between the Fermi energy and the mobility edge and  $\sigma_o$ , the conductivity at the mobility edge. In Figure 6, the natural logarithm of the conductivity of the samples is presented as a function of the inverse of temperature. Plotting the experimental data, the band gap energy  $E_g$  can be estimated (Table 3).

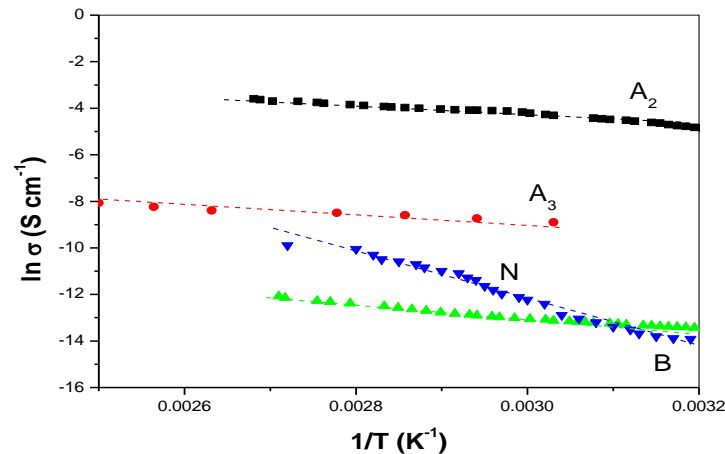


**Figure 6.** Ln conductivity ( $\sigma$ ) as a function of the inverse of temperature

The slopes were obtained by a linear fitting data at temperatures up to Table 3 shows the room conductivity ( $\sigma_{RT}$ ) and the calculated  $E_g$  values of OATA samples doped with different dopant ratio (see Table 1).

Table 3: conductivity and band gap energy of the studied samples

Sample	OATA (N)	OATA (B)	OATA (A3)	OATA (A2)	OATA (A1)
( $\sigma_{RT}$ ) Conductivity (S/cm)	1.3 10 <sup>-6</sup>	2.2 10 <sup>-6</sup>	1.8 10 <sup>-4</sup>	7.10 <sup>-3</sup>	4.5 10 <sup>-5</sup>
$E_g$ (ev)	1.6	0.52	0.42	0.40	-
$R^2$	0.9851	0.9838	0.9862	0.9870	-

$\sigma_{RT}$ : room temperature conductivity,  $E_g$ : band gap energy,  $R^2$ : fitting parameter

Acid dopant enhances conductivity. The best HCl/OATA ratio seems to be 2 (A2) as conductivity raises to 7.10<sup>-3</sup> S/cm while the undoped sample (N) shows three order lower conductivity values (1.3 10<sup>-6</sup> S/cm). It is interesting to remark that all samples show different temperature dependence.

Recently, heterocycles such as 1H-1,2,3-triazole has drawn interest as an alternative for use in proton exchange membrane fuel cells (PEMFCs) due to its electrochemical stability and high proton conductivity. Zhou et al. demonstrated apparently that a pronounced increase in conductivity was observed in vinyl-based polymers when the heterocyclic group was changed from an imidazole moiety to a triazole moiety [20]. Similar results were reported with imidazol [21] and with benzimidazole [22,23]. However, we measured the electrical property of the monomer 3-amino-1,2,4-triazole at room temperature and the results show high resistance values (> 103 M $\Omega$ ) related to an insulator.

#### III.4 Optical characterization of films

Optical experiments provide a good way of examining the properties of semiconductors, particularly measuring the absorption coefficient for various energies gives information about the band gaps of the material. Knowledge of these band gaps is extremely important for understanding the electrical properties of a semiconductor, and is therefore of great practical interest. The absorption edge or band edge is defined as the transition between the strong short-wavelength and the weak long-wavelength absorption in the spectrum of a solid, generally a semiconductor. The spectral position of this edge is determined by the energy separation

between the valence and conduction bands of the material in question. In the case of transparent solids, the absorption edge can be measured using transmittance techniques.

When the energy of the incident photon exceeds the band gap energy ( $E_g$ ) of the material, an electron is excited from the valence band to the conduction band [24]. In the parabolic band structure, the band gap  $E_g$  and absorption coefficient  $\alpha$  of a direct band gap semiconductor are related through the well known equation [25]

$$\alpha h\nu = C_1 (h\nu - E_g)^{1/2} \quad (2)$$

Where  $\alpha$  is the linear absorption coefficient of the material,  $h\nu$  is the photon energy and  $C_1$  is proportionality constant. Figure 6 shows  $(\alpha h\nu)^2$  versus  $h\nu$  plot of absorption spectrum of the undoped organic OATA oligomer. The best linear relationship is obtained by plotting  $(\alpha h\nu)^2$  against  $h\nu$  indicating that the optical band gap of this polymer is due to a direct allowed transition. The value of the band gap is determined from the intercept of the straight line at  $\alpha = 0$ , which is found to be 1.7 eV. This experimental value is similar than the calculated value presented in Table 3 for the undoped sample.

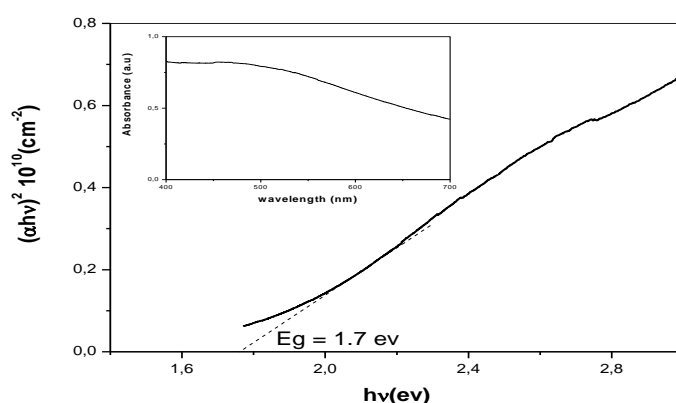


**Figure 6** Plot of  $(\alpha h\nu)^2$  versus  $h\nu$  (inset: Absorbance versus wavelength spectra) of OATA films of thickness 690 nm

#### IV. CONCLUSIONS

OATA samples show a semiconductor behavior in the temperature range of  $300\text{K} \leq T \leq 370\text{K}$ . It can be observed that the conductivity behavior of OATA is highly dependent on doping. The room temperature conductivity of OATA (N) and OATA (B) are similar, however acid dopant enhances conductivity. The best HCl/OATA ratio seems to be 2 (A2) as conductivity raises to  $7.10^{-3}$  S/cm while the undoped sample (N) shows three order lower conductivity values ( $1.3 \cdot 10^{-6}$  S/cm). Sample A2 shows the highest molecular order. This structure suggests good interchain connection without discarding ionic interchain conductivity. Further experiences are in progress.

From the UV-visible studies the band gap of neutral OATA film coated glass substrate is calculated. The result shows that the energy at which absorption starts corresponds to the direct band gap at 1.7 eV. For the reason that the organic semiconductor OATA may be used to prepare large-area thin film and flexible device on low-price, flexible substrates by means of solution method, the authors deduce that may have an important application potential in UV-Vis optoelectronic detecting or lighting field

#### ACKNOWLEDGEMENTS

The authors gratefully acknowledge the financial support from CONICET PIP 112-200801-00064), Agencia Nacional de Promoción Científica y Tecnológica (ANPCyT, project 2007-00291) and UBA are gratefully acknowledged. The authors thank CONICET for the fellowship to M.E.L. Dr. N. B. D. is a research member of CONICET.

#### REFERENCES

- [1]. W. Brutting. *Physics of Organic Semiconductors*. Wiley-VCH. 2005.
- [2]. T. A. Skotheim, J. Reynolds. *Handbook of Conducting Polymers*. 3rd Ed. Taylor & Francis. 2007.
- [3]. J. L. Atwood, J. W. Steed. *Organic Nanostructures*. Wiley-VCH. 2008.
- [4]. A. G. Davies, J. M. T. Thompson. *Advances in Nanoengineering: Electronics, Materials and Assembly*. Imperial College Press. 2007.
- [5]. V. Erokhin, M. K. Ram, O. Yavuz. *The New Frontiers of Organic and Composite Nanotechnology*. Elsevier. 2007.

- [6]. H. Sasabe. *Hyper-structured Molecules II: Chemistry, Physics and Applications*. Vol. 2. Gordon and Breach. 2001.
- [7]. W. R. Salneck, I. Lundstrom, B. Ranby. *Conjugated polymers and related Materials: The interconnection of Chemical and Electronic Structure*. Oxford Science. 1993.
- [8]. W. S. Huang, B. D. Humphrey, A. G. MacDiarmid, *J. Chem. Soc. Faradays Trans. I* 82 (1986) 2385.
- [9]. A. G. MacDiarmid, J. C. Chiang, M. Halpern, W. S. Huang, S. L. Mu, N. L. D. Somasiri, W. Wu, S. I. Yaniger. "Polyaniline": interconversion of metallic and insulating forms. *Mol. Cryst. Liq. Cryst.* 121 (1985) 173.
- [10]. Z. Sun, Y. Geng, J. Li, X. Jing, F. Wang. *Chemical polymerization of aniline with hydrogen peroxide as oxidant. Synth. Met.* 84 (1–3) (1997) 99.
- [11]. D. Zhang. *On the conductivity measurement of polyaniline pellets. Polym. Test.* 26 (2007) 9.
- [12]. Ş. Özden, S. Ü. Çelik, A. Bozkurt. *Synthesis and proton conductivity studies of doped azole functional polymer electrolyte membranes Electrochim. Acta*, doi:10.1016/j.electacta.2010.07.082 (2010) .
- [13]. D.C. Look, "Recent advances in ZnO materials and devices" *Materials Science and Engineering: B, Volume 80, Issues 1–3* (2001) 383
- [14]. M.E. Nicho, C.H. García-Escobar, D. Hernández-Martínez, I. Linzaga-Elizalde, G. Cadenas-Pliego, *Mater. Science and Engineering B* 161 (2009) 104
- [15]. M. E. Lamanna, E. de la Horra, S. Jacobo, N. B. D'Accorso. *Synthesis of an organic semiconductor by polymerization of 3-amino-1,2,4-triazole. React. Funct. Polym.* 69 (2009) 759.
- [16]. M. E. Lamanna, E. de la Horra, J. Sanabria, S. E. Jacobo, N. B. D'Accorso. *Acid-base behavior of an oligomer of 3-amino-1,2,4-triazole. J. of Appl. Polymer Sci., Vol. 123, Issue 5,* (2012) 2768
- [17]. – J. C. Apesteguy, S. E. Jacobo, *J.Mater. Sci* 42, 17 (2007), 7062
- [18]. T. Holstein. II. *Small polaron. Ann. Phys.* 8 (1959) 343.
- [19]. N. F. Mott, E. A. Davis. *Electronic Processes in Non-Crystalline Materials*. Oxford: Clarendon Press. 1979.
- [20]. Zhou, Z.; Li, S. W.; Zhang, Y. L.; Liu, M. L.; Li, W. *J Am Chem Soc* 127 (2005) 10824
- [21]. G. Scharfenberger; W. H Meyer; G. Wegner, M. Schuster; K. D. Kreuer; J. Maier, *Fuel Cells* 6 (2006) 237
- [22]. J. C. Persson, P. Jannasch, *Chem Mater* 18 (2006) 3096.
- [23]. J. C Persson; P. Jannasch, *Solid State Ionics* 177 (2006) 653.
- [24]. G.C. Bhar and R.C. Smith, *Phys. Stat. Sol. (b)*, 13 (1972) 157
- [25]. R.A.Smith, *In: Semiconductors, 2nd ed., Cambridge University Press, Cambridge*, 1978